Orig Life Evol Biosph (2008) 38:139–148
DOI 10.1007/s11084-008-9126-5

PREBIOTIC CHEMISTRY

Hydrothermal Stability of Adenine Under Controlled Fugacities of N_2, CO_2 and H_2

Michael Franiatte · Laurent Richard · Marcel Elie · Chinh Nguyen-Trung · Erwan Perfetti · Douglas E. LaRowe

Received: 7 January 2008 / Accepted: 4 February 2008 /
Published online: 23 February 2008

Abstract An experimental study has been carried out on the stability of adenine (one of the five nucleic acid bases) under hydrothermal conditions. The experiments were performed in sealed autoclaves at 300°C under fugacities of CO_2, N_2 and H_2 supposedly representative of those in marine hydrothermal systems on the early Earth. The composition of the gas phase was obtained from the degradation of oxalic acid, sodium nitrite and ammonium chloride, and the oxidation of metallic iron. The results of the experiments indicate that after 200 h, adenine is still present in detectable concentration in the aqueous phase. In fact, the concentration of adenine does not seem to be decreasing after ~24 h, which suggests that an equilibrium state may have been established with the inorganic constituents of the hydrothermal fluid. Such a conclusion is corroborated by independent thermodynamic calculations.

Keywords Adenine · Hydrothermal stability · Redox conditions · Thermodynamics · Fugacities

Introduction

Defining the temperature, pressure, and oxidation-reduction conditions under which organic nitrogen compounds are stable is of fundamental importance to the understanding of such

M. Franiatte · L. Richard (✉) · M. Elie · C. Nguyen-Trung
Nancy-Université, G2R, BP 239, 54506 Vandoeuvre-les-Nancy cedex, France
e-mail: laurent.richard@g2r.uhp-nancy.fr

E. Perfetti
Division Géologie–Géochimie–Géophysique, Institut Français du Pétrole, 1-4 avenue de Bois-Préau, 92852 Rueil-Malmaison cedex, France

D. E. LaRowe
Department of Earth Sciences—Geochemistry, Faculty of Geosciences, Utrecht University, P.O. Box 80.021, TA 3508 Utrecht, The Netherlands

processes as the formation of these compounds on the early Earth or the metabolism of hyperthermophilic microbes in present-day hydrothermal vents. Among these compounds, those which have received most of the attention from both experimental and theoretical studies are the amino acids, either for their synthesis from inorganic precursors (Hennet et al. 1992; Marshall 1994; Schoonen et al. 1999; Amend and Shock 1998, 2000) or their hydrothermal stability (Miller and Bada 1988; Shock 1990; Andersson and Holm 2000). In contrast, few experimental studies have been reported on the synthesis or thermal stability of the nucleic acid bases under hydrothermal conditions. Adenine was first synthesized by Oró (1961) from hydrogen cyanide (HCN) at 130°C under conditions supposedly representative of those on the early Earth. The purpose of the present communication is to report an investigation of the hydrothermal stability of adenine under controlled fugacities of CO_2, N_2, and H_2 and present a thermodynamic analysis of the results.

Experimental

Experimental Setup

Five experiments with different durations between 2 and 192 h have been conducted in stainless steel reactors at 300°C. The total pressure, which is internally generated, has been recalculated at the end of the experiments from compositional constraints using an equation of state (see below).

The type of reactor used in the experiments is represented in Fig. 1. It was originally designed by Nguyen-Trung et al. (1980) to carry out hydrothermal experiments in the $MgO–SiO_2–HCl–H_2O$ system. The reactors are cylindrical in shape, and have an internal volume of 15 cm^3. Their internal part is covered by a thin gold sheet, which is itself covered by a thin gold disk. The reactor is closed by a stainless steel lid, which is held with bolts tightened at 10 kg m with a dynamometric spanner.

A solution of $5{\cdot}10^{-3}$ mol of adenine (Acros Chemicals, >99.5%) was prepared with HPLC Chromanorm VWR™ water. Volumes of 10 cm^3 of that solution were introduced into each reactor. The $CO_2–N_2–H_2$ gas phase was generated in situ using a method similar

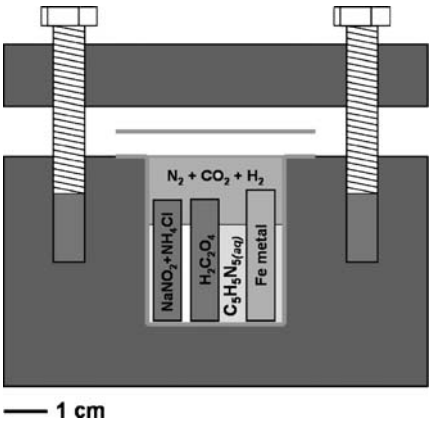

Fig. 1 Schematic representation of the reactor used in the experiments

to that proposed by Holloway and Reese (1974). Carbon dioxide was generated from the thermal decomposition of oxalic acid (RP Normapur™ Prolabo, 99.8%) according to

$$H_2C_2O_4 \rightarrow CO_2 + CO + H_2O \quad (1)$$

Under the experimental conditions considered in the present study, carbon monoxide should react with water to produce more CO_2 and H_2 in accord with the water–gas shift reaction (McCollom et al. 1999):

$$CO + H_2O \rightarrow CO_2 + H_2 \quad (2)$$

Nitrogen was obtained as follows (Hackspill et al. 1964). Sodium nitrite (Sigma Aldrich®, 99.5%) and ammonium chloride (Aldrich®, >99.5%) were reacted to yield ammonium nitrite and sodium chloride according to

$$NaNO_2 + NH_4Cl \rightarrow NH_4NO_2 + NaCl \quad (3)$$

the subsequent decomposition of ammonium nitrite yielding nitrogen and water according to

$$NH_4NO_2 \rightarrow N_2 + 2H_2O \quad (4)$$

Finally, hydrogen was produced in the experiments as a by-product of the oxidation of metallic iron (RP Normapur™ Prolabo, >99.5%) to magnetite according to

$$3Fe + 4H_2O \rightarrow Fe_3O_4 + 4H_2 \quad (5)$$

Oxalic acid and the mixture of sodium nitrite and ammonium chloride were inserted in two platinum cells welded at one end and pinched at the other end. Metallic iron was inserted in a gold cell also welded at one end and pinched at the other end. The amounts of reactants introduced in the different cells are given in Table 1.

High Performance Liquid Chromatography

The concentrations of adenine remaining at the end of each experiment were immediately measured by high performance liquid chromatography (HPLC) using a Hewlett Packard HP Series 1100 chromatograph. The method used in the present study is that described by Kießling et al. (2004). In this method, the compounds to be analyzed are separated on a RP-18 column using as a mobile phase a 0.02 molal solution of ammonium acetate (Aldrich ReagentPlus™, ≥99.99%) containing 5% volume of acetonitrile (Carlo Erba Reagenti,

Table 1 Reactant quantities (expressed in grams) used to generate the CO_2–N_2–H_2 gas phase

Experiment (h)	$H_2C_2O_4$	NH_4Cl	$NaNO_2$	Iron metal
2	0.2756	0.1788	0.1716	~2
24	0.2183	0.1751	0.1661	~2
96	0.1765	0.1683	0.1671	~2
120	0.1956	0.1594	0.1592	~2
192	0.1858	0.1660	0.1630	~2

99.9%). This solution was prepared with HPLC Chromanorm VWR™ water. The pH of the solution was approximately equal to 6.

A calibration line was established by preparing a series of solutions of adenine corresponding to concentrations of 0.1, 0.05, 0.01, 0.005, 0.001, and 0.0005 g l^{-1}. An internal standard of thymidine (Sigma Aldrich®, 99%) with a concentration of 0.005 g l^{-1} was introduced into each of the adenine solutions.

The solutions of adenine were injected manually in the chromatograph with a syringe. The injected volumes were equal to 20 μl. The flow rate of the mobile phase was fixed at 1 ml min^{-1}. All measurements have been performed at 25°C and a pressure of 166 bar.

Results

The reactors were successively removed from the oven after 2, 24, 96, 120, and 192 h, and opened at room temperature after approximately 1 day of cooling. The initial volumes of aqueous solution and those recovered after the experiments are given in Table 2, along with the concentrations of adenine remaining at the end of each experiment. Both concentrations directly measured by HPLC (C_{ad} meas.) and corrected concentrations (C_{ad} corr.) are reported in Table 2. A correction is necessary since H_2O is respectively produced in Reactions 1 and 4, but consumed in Reactions 2 and 5 as well as in the reaction of decomposition of adenine (see Reaction 7 below). The corrected concentrations were obtained from

$$C_{\mathrm{ad}}\,\mathrm{corr.} = C_{\mathrm{ad}}\,\mathrm{meas.} \cdot \frac{V_f}{V_i} \tag{6}$$

where V_f and V_i represent the final and initial volumes of adenine solution. The HPLC analyses for adenine concentrations were repeated three times or more, which resulted in the uncertainties shown in Table 2.

The corrected concentrations of adenine have been plotted against the duration of the experiments in Fig. 2. It can be seen in this figure that the concentration of adenine rapidly dropped from the initial concentration of $5{\cdot}10^{-3}$ mol l^{-1} to a value of ~$9{\cdot}10^{-6}$ mol l^{-1} after 24 h, after which this concentration appears to be slowly decreasing towards an essentially constant value. The evolution of the adenine concentration (C_{adenine}) as a function of time (t) can be tentatively described by an exponential decay function written as

$$\mathrm{C_{adenine}} = \left(7.237 \cdot 10^{-6}\right) + \left(4.993 \cdot 10^{-3}\right)\mathrm{e}^{-2.558\mathrm{t}} \tag{7}$$

Table 2 Initial volumes (V_i) of solution and final volumes (V_f) remaining at the end of each experiment, and adenine concentrations measured (C_{ad} meas.) and corrected (C_{ad} corr.) for the loss of water during the experiments (see text)

Time (h)	V_i (ml)	V_f (ml)	C_{ad} meas. (mol/l)	C_{ad} corr. (mol/l)
0	10	–	5.0×10^{-3}	–
2	10	5.60	$6.643\pm0.829\times10^{-5}$	$3.720\pm0.464\times10^{-5}$
24	10	8.30	$1.078\pm0.391\times10^{-5}$	$0.895\pm0.325\times10^{-5}$
96	10	5.34	$1.287\pm0.352\times10^{-5}$	$0.687\pm0.188\times10^{-5}$
120	10	5.20	$1.763\pm0.402\times10^{-5}$	$0.917\pm0.209\times10^{-5}$
192	10	8.60	$0.461\pm0.283\times10^{-5}$	$0.396\pm0.244\times10^{-5}$

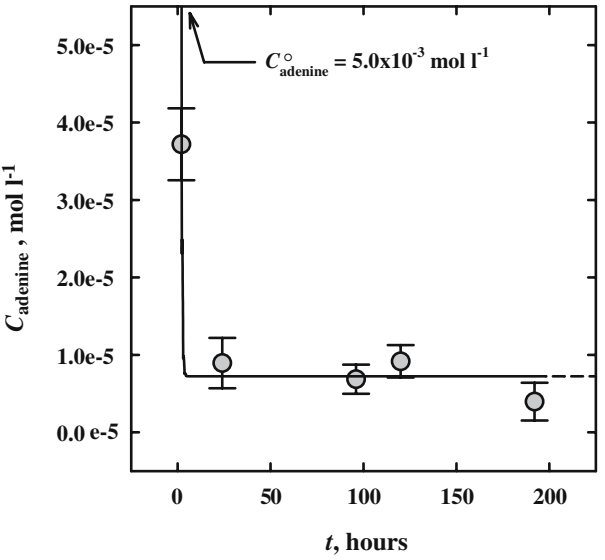

Fig. 2 Evolution of the concentration of adenine in the aqueous solution as a function of reaction time. The symbols correspond to the corrected concentrations listed in Table 2. The curve is consistent with Eq. 7

where the $7.237 \cdot 10^{-6}$ mol l^{-1} value would represent the equilibrium concentration at infinite time. Equation (7), which corresponds to the curve shown in Fig. 2, should be considered with caution. It only represents an adjustment to the experimental data and would be consistent with attainment of an equilibrium state after ~5 h, which is probably largely underestimated.

X-ray diffraction patterns of the reacted iron metal after 24 and 192 h are shown in Fig. 3. It can be seen in this figure that magnetite progressively replaces iron metal, which has nearly disappeared after 192 h of reaction. This observation puts some constraints on the hydrogen fugacity obtained at the end of the latter experiment. It can be deduced from the logarithmic fugacity diagram depicted in Fig. 4 that the stability field of magnetite at 300°C and 250 bars correspond to hydrogen fugacity values between $\sim 10^{-2.2}$ and $10^{3.3}$ bars, and fugacities of CO_2 lower than $\sim 10^{1.0}$ bars and $10^{2.8}$ bars.

The fact that adenine concentrations do not seem to be decreasing to an appreciable degree after ~24 h of reaction suggests that adenine may have approached an equilibrium state with the inorganic constituents of the hydrothermal fluid. The hypothesis that an equilibrium state may have been approached in our experiments is evaluated in the thermodynamic analysis presented below.

Thermodynamic Interpretation

Metastable equilibrium between aqueous adenine, liquid water, gaseous carbon dioxide, hydrogen, and nitrogen can be written as

$$C_5H_5N_{5(aq)} + 10H_2O_{(l)} = 5CO_{2(g)} + 12.5H_{2(g)} + 2.5N_{2(g)} \quad (8)$$

where the (aq), (l), and (g) subscripts denote the aqueous, liquid, and gas states, respectively. The logarithm of the equilibrium constant [log $K_{(8)}$] of Reaction 8 has been computed at 300°C and 250 bars (see below) with the SUPCRT92 computer program (Johnson et al. 1992) and values for the standard molal thermodynamic properties and

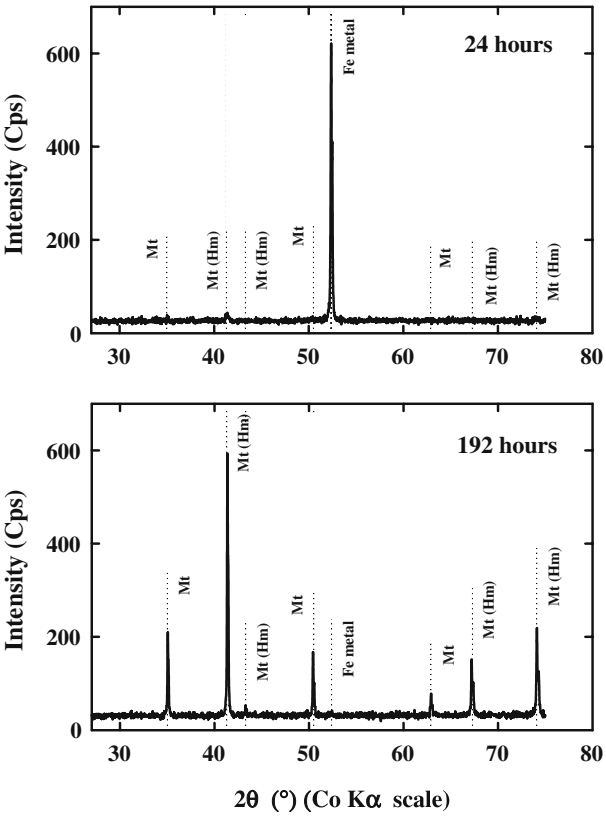

Fig. 3 Powder X-ray diffractograms of the iron-bearing phases present in the gold capsules after 24 and 192 h. The peaks in the diffractograms correspond to the Bragg positions characteristic of iron (noted Fe metal) and magnetite (noted Mt). Although magnetite appears to be the sole product of iron oxidation in our experiments, peaks corresponding to diffraction by both magnetite and hematite are identified as Mt (Hm)

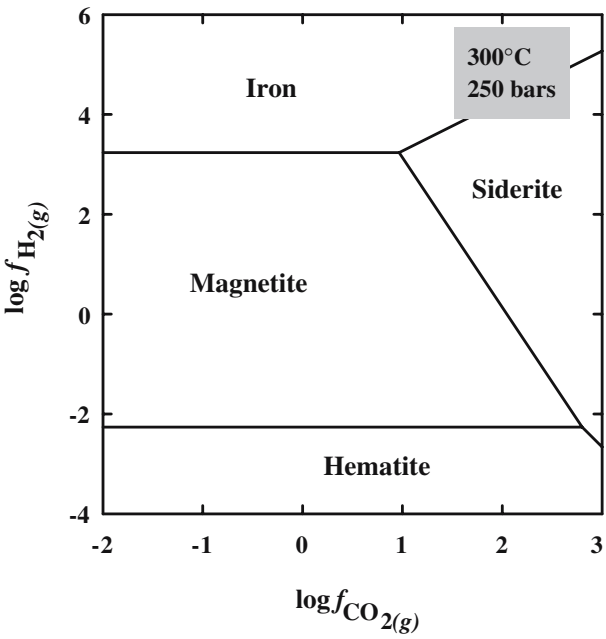

Fig. 4 Logarithmic $f_{CO_2(g)} - f_{H_2(g)}$ diagram showing the stability fields of iron metal, magnetite, hematite and siderite at 300°C and 250 bars. The stability limits between the various phases have been computed with the SUPCRT92 computer program (Johnson et al. 1992) adopting standard states of unit activities for the pure solids and liquid water

parameters for the revised Helgeson–Kirkham–Flowers (HKF) equation of state (Tanger and Helgeson 1988) taken from LaRowe and Helgeson (2006) for aqueous adenine. Assuming that the activity of liquid water in our experiments was approximately equal to one, the logarithmic analog of the law of mass action for Reaction 8 is given by

$$\log K_{(8)} = 5\log f_{CO_{2(g)}} + 12.5\log f_{H_{2(g)}} + 2.5\log f_{N_{2(g)}} - \log a_{C_5H_5N_{5(aq)}} = 45.376 \quad (9)$$

where $f_{CO_{2(g)}}$, $f_{H_{2(g)}}$, and $f_{N_{2(g)}}$ designate the fugacities of gaseous CO_2, H_2 and N_2, and $a_{H_2O_{(l)}}$ and $a_{C_5H_5N_{5(aq)}}$ represents the activity of aqueous adenine.

Equation 9 has been used to construct the fugacity diagrams shown in Fig. 5, in which the logarithm of the fugacity of CO_2 gas has been plotted as a function of that for N_2 gas. The solid lines correspond to logarithmic contours of the activity of adenine in the hydrothermal solution, which were computed in the different diagrams for hydrogen gas fugacities equal to 1, 10, 100, and 1,000 bars. It can be deduced from these fugacity diagrams that detectable concentrations of aqueous adenine can only be in equilibrium with

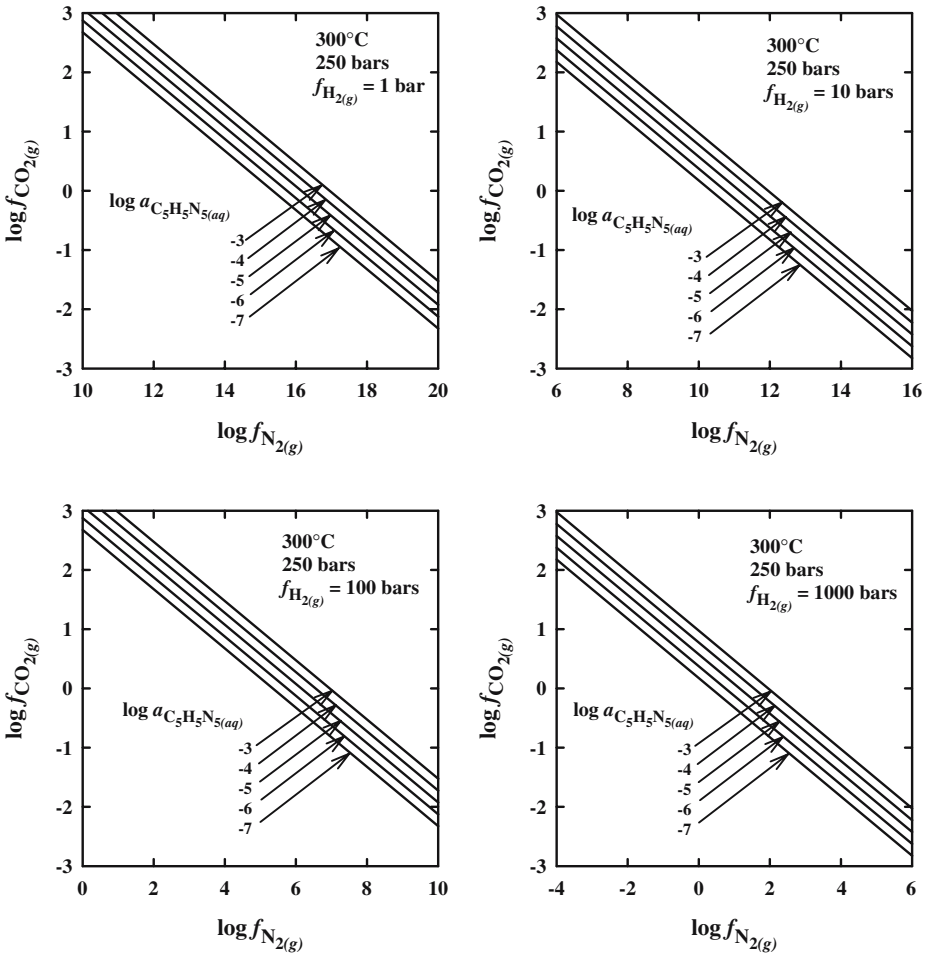

Fig. 5 Logarithmic $f_{N_{2(g)}} - f_{CO_{2(g)}}$ fugacity diagrams at 300°C and 250 bars at fixed $f_{H_{2(g)}}$ values. The straight lines in the diagram correspond to logarithmic contours of the activity of adenine computed from Eq. 9

CO_2, N_2, and H_2O for hydrogen fugacities between 100 and 1,000 bars. Lower values of $f_{H_{2(g)}}$ result in physically unattainable fugacities of N_2 gas.

The fugacity f_i of a volatile species in a fluid mixture (i.e.) is defined by

$$f_i = \varphi_i \cdot x_i \cdot P \tag{10}$$

where φ_i and x_i stand for the fugacity coefficient and mole fraction of the subscripted species in the mixture, respectively, and P is the total pressure. Values for the fugacities of CO_2, N_2, H_2 and H_2O have been estimated for our experimental conditions using Soave's (1972) modification of the Redlich–Kwong equation of state (Redlich and Kwong 1949). This equation of state is written for a pure fluid as

$$P = \frac{RT}{(V-b)} - \frac{a(T)}{V(V+b)} \tag{11}$$

where P is again the total pressure (bar), R is the gas constant (8.314472 J mol^{-1} K^{-1}), T is the absolute temperature (K), V is the molar volume of the fluid mixture (cm^3 mol^{-1}), and b and $a(T)$ are the van der Waals parameters. The $a(T)$ parameter is temperature-dependent in Soave's (1972) equation, and is written as a function of the acentric factor ω.

The fugacity coefficient of the ith species in the fluid (φ_i) is related to the compressibility factor (z) by (Prausnitz et al. 1986):

$$\ln \varphi_i = \int_0^P \frac{z-1}{P} \mathrm{d}P \tag{12}$$

Equations 11 and 12 have been combined and solved together with values of the a, b and ω parameters taken from Prausnitz et al. (1986), mixing rules given by Soave (1972), binary interaction coefficients derived from phase equilibria studies, and mole fractions obtained from the stoichiometries of Reactions 1, 2, 3, 5, and 8 and the amounts of reactants used in the longest experiment (192 h). The values obtained for the fugacity coefficients and fugacities of CO_2, N_2, H_2, and H_2O at a total pressure of 250 bars (which is specified in the fugacity calculation) are listed in Table 3. It can be deduced from this table that the fugacities computed for H_2 and CO_2 plot within the stability field of magnetite in Fig. 4, in agreement with the results of the X-ray diffraction analysis. Combining the values of the fugacities for CO_2, N_2, and H_2 with Eq. 9 results in

$$a_{C_5H_5N_{5(aq)}} \sim 6.9 \cdot 10^{-6}, \tag{13}$$

Table 3 Mole fractions, fugacity coefficients, fugacities, and partial pressures computed at 300°C and 250 bars from the Soave–Redlich–Kwong equation of state together with compositional constraints based on the experiment at 192 h (see text)

Species	x_i[a]	φ_i[a]	f_i[b]	p_i[b]
CO_2	0.008	3.97	8.4	2.1
N_2	0.005	18.49	22.2	1.2
H_2	0.102	14.89	378.6	25.4
H_2O	0.885	0.36	80.3	221.3

[a] Dimensionless

[b] Bar

which is of the order of the adenine concentrations reported in Table 2. It should perhaps be emphasized here that the hydrogen fugacities of several hundred bars required to stabilize adenine at 300°C are more than two orders of magnitude higher than the value defined by the quartz–fayalite–magnetite buffer which is representative of the oxidation-reduction conditions in the peridotite-hosted hydrothermal systems of the Mid-Atlantic Ridge (Holm and Charlou 2001). Although these hydrothermal systems have been proposed as analogues for Archean hydrothermal systems, it appears that the stabilization (and therefore the synthesis) of organic compounds of prebiotic interest at high temperature would have required much more reducing conditions than those prevailing in present-day hydrothermal systems.

Conclusion

The thermal decomposition of adenine in aqueous solution at 300°C has been studied experimentally under in situ generated fugacities of CO_2, N_2, and H_2. The concentration of adenine decreased rapidly during the first 24 h of the experiment, then kept decreasing slowly. Adenine was still present in the hydrothermal solution after ~200 h at a concentration of the order of $4 \cdot 10^{-6}$ mol l^{-1}. The change of decomposition rate may be attributable to the approach of an equilibrium state with the inorganic constituents of the hydrothermal solution, an hypothesis which is confirmed by a thermodynamic analysis of the experimental results.

References

Amend JP, Shock EL (1998) Energetics of amino acid synthesis in hydrothermal ecosystems. Science 281:1659–1662

Amend JP, Shock EL (2000) Thermodynamics of amino acid synthesis in hydrothermal systems on early Earth. In: GAM Goodfriend et al (ed) Perspectives in amino acid and protein geochemistry. Oxford, pp 23–40

Andersson E, Holm NG (2000) The stability of some selected amino acids under attempted redox constrained hydrothermal conditions. Orig Life Evol Biosph 30:9–23

Hackspill L, Besson J, Hérold A (1964) Chimie Minérale. Presses Universitaires de France

Hennet RJC, Holm NG, Engel MH (1992) Abiotic synthesis of amino acids under hydrothermal conditions and the origin of life: a perpetual phenomenon? Naturwissenschaften 79:361–365

Holloway JR, Reese RL (1974) The generation of N_2–CO_2–H_2O fluids for use in hydrothermal experimentation. I. Experimental method and equilibrium calculations in the C–O–H–N system. Amer Mineral 59:587–597

Holm NG, Charlou JL (2001) Initial indications of abiotic formation of hydrocarbons in the Rainbow ultramafic hydrothermal system, Mid-Atlantic Ridge. Earth Planet Sci Lett 191:1–8

Johnson JW, Oelkers EH, Helgeson HC (1992) SUPCRT92: A software package for calculating the standard molal thermodynamic properties of minerals, gases, aqueous species, and reactions from 1 to 5000 bar and 0 to 1000°C. Comput Geosci 18:899–947

Kießling P, Scriba GKE, Süß, F, Werner G, Knoth H, Hartmann M (2004) Development and validation of a high-performance liquid chromatography assay and a capillary electrophoresis assay for the analysis of adenosine and the degradation product adenine in infusions. J Pharm Biochem Anal 36:535–539

LaRowe DE, Helgeson HC (2006) Biomolecules in hydrothermal systems: calculation of the standard molal thermodynamic properties of nucleic-acid bases, nucleosides, and nucleotides at elevated temperatures and pressures. Geochim Cosmochim Acta 70:4680–4724

Marshall WL (1994) Hydrothermal synthesis of amino acids. Geochim Cosmochim Acta 58:2099–2106

McCollom TM, Ritter G, Simoneit BRT (1999) Lipid synthesis under hydrothermal conditions by Fischer–Tropsch-type reactions. Orig Life Evol Biosph 29:153–166

Miller SL, Bada JL (1988) Submarine hot springs and the origin of life. Nature 334:609–611

Nguyen-Trung C, Pichavant M, Weisbrod A (1980) Contribution à l'étude expérimentale du système $MgO–SiO_2–HCl–H_2O$. In: Besson M (ed) Facteurs contrôlant les minéralisations sulfurées de nickel. Editions BRGM, pp 253–263

Oró J (1961) Mechanism of synthesis of adenine from hydrogen cyanide under possible primitive Earth conditions. Nature 191:1193–1194

Prausnitz JM, Lichtenthaler RN, de Azevedo EG (1986) Molecular thermodynamics of fluid-phase equilibria, 2nd edn. Prentice-Hall

Redlich O, Kwong JNS (1949) On the thermodynamics of solutions. V. An equation of state. Chem Phys 44:233–244

Schoonen MAA, Xu Y, Bebie J (1999) Energetics and kinetics of the prebiotic synthesis of simple organic acids and amino acids with the $FeS–H_2S/FeS_2$ redox couple as reductant. Orig Life Evol Biosph 29:5–32

Shock EL (1990) Do amino acids equilibrate in hydrothermal fluids? Geochim Cosmochim Acta 54: 1185–1189

Soave G (1972) Equilibrium constants from a modified Redlich–Kwong equation of state. Chem Eng Sci 27:1197–1203

Tanger JC, Helgeson HC (1988) Calculation of the thermodynamic and transport properties of aqueous species at high pressures and temperatures; revised equations of state for the standard partial molal properties of ions and electrolytes. Amer J Sci 288:19–98